Journal of Hazardous Materials 398 (2020) 123002

Contents lists available at ScienceDirect

Journal of Hazardous Materials

journal homepage: www.elsevier.com/locate/jhazmat

Effect of methanethiol on process performance, selectivity and diversity of sulfur-oxidizing bacteria in a dual bioreactor gas biodesulfurization system

Karine Kiragosyan[a,b,*], Magali Picard[a,c], Peer H.A. Timmers[a,d], Dimitry Y. Sorokin[a,e,f], Johannes B.M. Klok[a,b,g], Pawel Roman[a], Albert J.H. Janssen[b,h]

[a] Wetsus, European Centre of Excellence for Sustainable Water Technology, Oostergoweg 9, 8911 MA Leeuwarden, the Netherlands
[b] Environmental Technology, Wageningen University & Research, P.O. Box 17, 6700 AA Wageningen, the Netherlands
[c] Eurofins Agroscience Services Chem SAS 75, chemin de Sommières 30310, Vergèze, France
[d] Laboratory of Microbiology, Wageningen University & Research, Wageningen, the Netherlands
[e] Winogradsky Institute of Microbiology, Research Centre of Biotechnology, Russian Academy of Sciences, Prospect 60-let Oktyabrya 7/2, Moscow, Russian Federation
[f] Department of Biotechnology, Delft University of Technology, Van der Maasweg 9, 2629 HZ, Delft, the Netherlands
[g] Paqell B.V., Reactorweg 301, 3542 AD, Utrecht, the Netherlands
[h] Shell, Oostduinlaan 2, 2596 JM, the Hague, the Netherlands

GRAPHICAL ABSTRACT

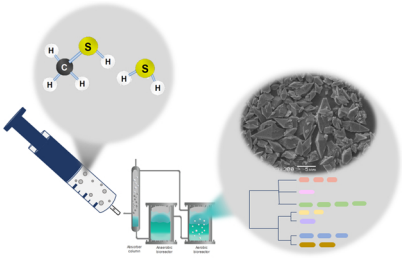

ARTICLE INFO

Editor: R. Teresa

Keywords:
Thiol toxicity
Thioalkalibacter halophilus
Alkalilimnicola ehrlichii
Thioalkalivibrio sulfidiphilus
Microbial dynamics

ABSTRACT

This study provides important new insights on how to achieve high sulfur selectivities and stable gas biodesulfurization process operation in the presence of both methanethiol and H_2S in the feed gas. On the basis of previous research, we hypothesized that a dual bioreactor lineup (with an added anaerobic bioreactor) would favor sulfur-oxidizing bacteria (SOB) that yield a higher sulfur selectivity. Therefore, the focus of the present study was to enrich thiol-resistant SOB that can withstand methanethiol, the most prevalent and toxic thiol in sulfur-containing industrial off gases. In addition, the effect of process conditions on the SOB population dynamics was investigated. The results confirmed that thiol-resistant SOB became dominant with a concomitant increase of the sulfur selectivity from 75 mol% to 90 mol% at a loading rate of 2 mM S methanethiol day^{-1}. The abundant SOB in the inoculum – *Thioalkalivibrio sulfidiphilus* – was first outcompeted by *Alkalilimnicola ehrlichii* after which *Thioalkalibacter halophilus* eventually became the most abundant species. Furthermore, we found that the actual electron donor in our lab-scale biodesulfurization system was polysulfide, and not the primarily supplied sulfide.

* Corresponding author at: Wetsus, European Centre of Excellence for Sustainable Water Technology, Oostergoweg 9, 8911 MA, Leeuwarden, the Netherlands.
E-mail addresses: karinekiragosyan@gmail.com, karine.kiragosyan@wetsus.nl (K. Kiragosyan).

https://doi.org/10.1016/j.jhazmat.2020.123002
Received 14 March 2020; Received in revised form 30 April 2020; Accepted 19 May 2020
Available online 24 May 2020

1. Introduction

Among many reduced sulfur compounds, natural gas and landfill gas streams may contain thiols (RSH) and hydrogen sulfide (H_2S) at high concentrations. Thiols and H_2S need to be removed because of their obnoxious smell and low odor threshold values, their contribution to atmospheric pollution as well as their toxicity and corrosive nature (Chen et al., 2017). Various techniques are available for the simultaneous removal of these compounds, such as physicochemical acid/alkali scrubbing (Smet et al., 1998) and biological conversion (Syed et al., 2006). Important drawbacks of physicochemical methods for sour gas treatment are the formation of waste streams and the high operating costs, whereas biological conversion processes are environmentally friendly and more cost-effective (Cline et al., 2003). However, the latter still have room for further optimization.

In this paper, we present an upgraded gas biodesulfurization technology. It concerns the adsorption of thiols and H_2S in a highly buffered, moderately alkaline solution pH 8–10, followed by an oxidation step, in which haloalkaliphilic sulfide-oxidizing bacteria (SOB) convert sulfide to elemental sulfur as a major and sulfate as a minor products at low redox potential created by oxygen-limited conditions (Van Den Bosch et al., 2007). The formation of sulfur and sulfate is accompanied by the production of hydroxyl ions (OH^-) and protons (H^+), respectively. A small fraction of sulfide is chemically oxidized to thiosulfate (through intermediate polysulfide forming from sulfur and sulfide at high pH). Elemental sulfur, however, is the preferred end (insoluble and easily separated) product as the associated regeneration of hydroxide ions (needed for H_2S absorption) leads to a reduction in caustic (NaOH) consumption, hence in a decrease in air-oxygen requirements as well as energy requirements (Van Den Bosch et al., 2007).

When thiols are present in the feed gas along with H_2S, a sequence of complex abiotic reactions will take place, as the dissolved thiols (Eq. 1) will react with produced bio-sulfur particles (S_8) to form diorgano polysulfanes (DOPS) (Eq. 2). Diorgano pentasulfide is the dominant product (Roman et al., 2014), which subsequently decomposes into a mixture of organosulfur compounds (Eq. 3). Moreover, thiols will also be chemically oxidized in the presence of oxygen and form diorgano disulfides (Eq. 4)

$$RSH + OH^- \rightarrow RS^- + H_2O \quad (1)$$

$$2RS^- + S_8 \rightarrow RS_nR + S_x^{2-}, \text{ with } n + x = 10 \quad (2)$$

$$RS_nR \leftrightarrow RS_{n-1}R + RS_{n+1}CH_3, \text{ with } n > 3 \quad (3)$$

$$RSH + \tfrac{1}{2}\, O_2 \rightarrow RS_2R + H_2O \quad (4)$$

Previous studies revealed that the formation of biological sulfur is highly sensitive to the presence of thiols (Roman et al., 2016a; Van Den Bosch et al., 2009b) because of the associated inhibition of SOB. Roman et al. (2016c) tested the effects of various thiols and their oxidation products such as DOPS and found that microbial sulfide oxidation capacity was inhibited by short-chain thiols (methane-, ethane- and propanethiol) at concentrations as low as 0.6 μM. To make the biodesulfurization process more robust, the focus of that study was to enrich the biomass with thiol-resistant SOB that can withstand methanethiol (MT), the most prevalent and toxic thiol (Roman et al., 2016a). During two months of continuous process operation and at gradually increasing MT supply rates, Roman et al. (2016b) found that the initial SOB community undergone significant change resulting in the domination of a MT- resistant SOB species. However, the obtained sulfur selectivity was still low, i.e. 75 mol%, at 2 mM S day^{-1} of MT and 61.8 mM H_2S day^{-1}. (Throughout this paper, we use the term "selectivity" to refer to the mol fractions of the formed products.) Moreover, the process operation was unstable as the control of the O_2 supply, based on the oxidation-reduction potential (ORP), became unreliable.

To expand the operating window of the current gas biodesulfurization process and allow the combined treatment of H_2S and thiol-containing gas streams, we modified the process lineup by the addition of an anaerobic bioreactor. Based on our previous work, we hypothesized that creating anaerobic conditions in combination with aerobic conditions would affect the reduction-oxidation state of the sulfide-oxidizing enzymes flavocytochrome *c* and sulfide-quinone oxidoreductase (Klok et al., 2013; Ter Heijne et al., 2018). The first insights on the dual bioreactor process performance indeed showed an increase in sulfur selectivity up to 97 mol% when only H_2S was present in the feed gas (De Rink et al., 2019). This finding prompted us to investigate the effect of methanethiol on sulfur formation in the new dual bioreactor process. We monitored SOB community dynamics as part of our investigation to select and possibly identify prevalent MT-resistant SOB.

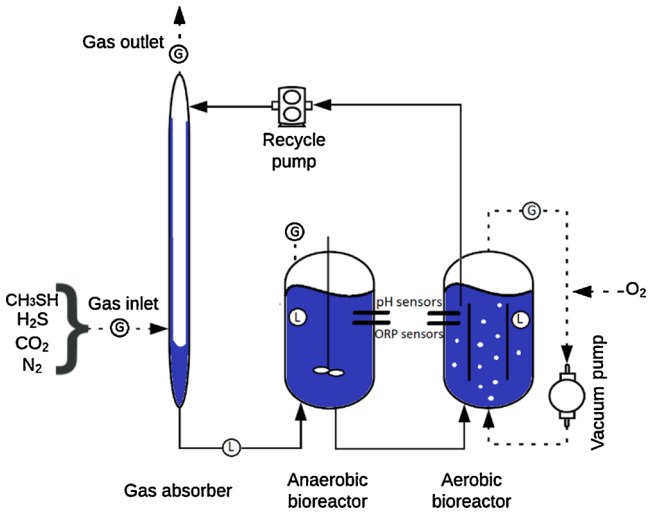

Fig. 1. Schematic representation of the experimental setup used for the experiments. G = gas sampling point, L = liquid sampling point, CH_3SH = methanethiol (MT). The blue area indicates liquid. (For interpretation of the references to colour in this figure legend, the reader is referred to the web version of this article.)

2. Materials and methods

2.1. Reactor operation

The experimental laboratory setup consisted of a falling film gas absorber followed by an anaerobic and aerobic bioreactor in series, operated in fed-batch mode (Fig. 1). A mixed gas stream consisting of three gases i.e. N_2, H_2S and MT was fed to the absorber at a total gas flow of 166 mL min^{-1}. H_2S and N_2 gases were constantly supplied, their volume fractions were 1.5% and 98.5% respectively. At the onset of MT addition, the gas flow of N_2 was proportionally reduced. For instance, the gas flow of MT was 2.5 mL min^{-1} and N_2 was 125.5 mL min^{-1}. MT flow fraction at this flow rate was equal to 0.015% to the total supplied gas. The CO_2 gas flow is pH-dependent, thus, excluded from the total gas flow as the CO_2 will dissolve in the aqueous phase. The gas retention time in the gas absorber is 27 s with gas velocity of 0.035 m s^{-1}, based on the absorber column diameter 0.011 m and height 0.8 m. In addition, specific gas-liquid interfacial area was 396 m^2 m^{3-}. The composition of the feed-gas was controlled with mass flow controllers (type EL-FLOW, model F-201DV-AGD-33-K/E, Bronkhorst, the Netherlands). For each type of gas, a mass flow controller was selected with an appropriate orifice to enable precise control of the required dosing rate. We used a 0-17 mL min^{-1} mass flow controller for the supply of hydrogen sulfide. The flow range was 0-350 mL min^{-1} for nitrogen, 0-30 mL min^{-1} for oxygen and 0-40 mL min^{-1} for carbon dioxide. Hydrogen sulfide and nitrogen gas were continuously supplied. The oxygen and carbon dioxide supply were controlled with a multiparameter transmitter (Liquiline CM442-1102/0, Endress+Hauser, Germany), which

was paired with an ORP sensor to control the oxygen supply (Orbisint 12D-7PA41; Endress + Hauser, Germany) and with a pH sensor to control the carbon dioxide supply (Orbisint 11D-7AA41; Endress + Hauser, Germany). A digital gear pump was used to assure liquid recirculation between the aerobic bioreactor and the gas absorber (EW-75211-30, Cole-Palmer, USA) at a constant flow of 10 L h^{-1}. A gas compressor (N-820 FT.18, KNF Laboport, NJ, USA) was used to recycle gas (20 L min^{-1}) over the aerobic bioreactor. The anaerobic bioreactor was equipped with a stirrer to ensure mixing. The gas absorber and the bioreactors' temperature were controlled at 35 °C by a thermostat bath (DC10, Thermo Haake, Germany).

Liquid samples were taken from three different sampling points (one located at the bottom section of the absorber, a second one in the anaerobic bioreactor and a third in the aerobic bioreactor; see Fig. 1). Gas-phase samples were taken from four different locations (gas inlet, both bioreactor headspaces and absorber outlet). Sampling was done in triplicate for liquid samples, while single samples were taken for gas analyses at regular time intervals. For microbial community analysis, a 100 mL aliquot from the aerobic bioreactor culture was centrifuged to obtain a cell pellet for further DNA extraction.

Two sets of experiments were conducted. In the first experiment, the system was fed continuously with only H_2S for 15 days to establish a baseline. Next, MT was stepwise supplied (0–2 mM S day^{-1}) over a 77-day period to allow SOB biomass to adapt to MT and to minimize the risk of toxification. Throughout the entire experiment, the H_2S supply was kept constant at 58.15 mM S day^{-1}. The liquid volume of the dual bioreactor setup was 5 L, but we only considered the active volume of the aerobic bioreactor in the mass balance calculations, i.e. 2.5 L (Table 1). The anaerobic bioreactor liquid volume equaled 2.3 L, while the remaining 0.2 L was distributed over the volume of the tubing and bottom section of the absorber column.

As the system was operated in fed-batch mode, the formed products (i.e. biosulfur particles, thiosulfate and sulfate) accumulated in the system during the experimental run. Each time the sulfur concentrations became too high, the system became more difficult to operate as a result of the inadequate separation of the liquid, gas and solid phases, resulting in the entrainment of sulfur particles in the recirculation gas stream. To prevent this, the sulfur content was lowered by a partial exchange of the medium; the aerobic bioreactor (2.5 L) was completely emptied and then replenished with fresh medium. Thus, medium was exchange on the day 12, 29 and 44, resulting in four operation time intervals: 1 = day 1–11, 2 = day 12–29, 3 = day 29–44, and 4 = day 44–47. Biomass was returned to the bioreactor after removal of the sulfur particles via centrifugation (20 min at 16,000 *g*). The haloalkaline medium was buffered with 0.045 M Na_2CO_3 and 0.91 M $NaHCO_3$. A detailed description of the medium can be found in Kiragosyan et al. (2019a). The pH of the medium was 8.5 ± 0.05 at 35 °C.

2.2. Inoculum

A "super mix" inoculum was prepared by mixing various biomass samples, originating from four different full-scale biodesulfurization installations, which we named Oilfield – 1, Oilfield – 2, Landfill and Pilot (Kiragosyan et al., 2019a, 2019b). "Oilfield – 1″ is a full-scale installation treating gas from oil production wells containing low concentrations of thiols (50–200 ppm) and 1–5% of H_2S, whereas "Oilfield – 2″ treats acid gas from an amine regeneration unit with 10–20% of H_2S and thiols (Kiragosyan et al., 2019a, 2019b). The "Landfill" installation treats landfill gas containing 0.3% of H_2S, and the "Pilot" treats synthetically prepared gas that represents amine acid gas with 4.45% of H_2S (De Rink et al., 2019). The biomasses and their proportions were chosen based on individual SOB biomass performance in previously performed experiments and SOB biomass community composition (Kiragosyan et al., 2020, 2019a, 2019b). The biomasses were mixed in the following volumetric proportion: 1:0.5:0.5:1 (Oilfield – 1: Oilfield – 2: Landfill: Pilot), followed by a centrifugation step (15 min at 16,000 *g*) to concentrate the suspended cells. The obtained cell pellet was used to inoculate a 5-L system (2.5 L per bioreactor).

The biomass mix served to inoculate the system for the first experimental run. After completing the first experiment, the developed biomass was harvested and used as inoculum for the second experiment.

Table 1
Overview of the process conditions of the performed experiments.

Parameter	Value
Active liquid volume, L	2.5
Total liquid volume, L	5
pH set-point	8.50 ± 0.05
Salinity, Na^+ M	1
Temperature set-point, °C	35 ± 1
H_2S loading, mM S day-^{1}	58.2
CH_3SH loading, mM S day-^{1}	0 – 2
ORP set-point, mV	−390

2.3. Microbial biomass sampling, sample preparation, and DNA extraction

During both experiments, SOB biomass samples were collected at equal time intervals. During the first experimental run with only H_2S addition, five samples were taken in triplicate over 15 days. In the second run, 15 samples were collected in triplicates over 77 days. The samples were first centrifuged (15 min at 16,000 *g*) to separate the biomass from the reactor suspension. Hereafter, the bacterial cells were resuspended and washed twice with a 0.5 M Na^+ bicarbonate buffer solution at pH 8.5. All 60 biomass samples were stored at -80 °C awaiting DNA extraction.

Genomic DNA was extracted using the DNeasy PowerLyzer PowerSoil Kit (Qiagen, the Netherlands/Germany) following the manufacturer's instructions. Extracted DNA was quantified using the QuantiFluor dsDNA system on a Quantus™fluorometer (Promega, the Netherlands). DNA integrity was evaluated with gel electrophoresis.

2.4. qPCR

qPCR was performed on all (60) samples from the experimental runs. Samples were analyzed based on the absolute abundance of the three SOB species of interest, namely *Alkalilimnicola ehrlichii, Thioalkalivibrio sulfidiphilus,* and *Thioalkalibacter halophilus,* by using specially developed species-specific primers (Kiragosyan et al., 2019b). For *Thioalkalivibrio sulfidiphilus*, primers were designed for a remote subcluster of this genus, as *Thioalkalivibrio sulfidiphilus* HL-EbGR7 is genetically related to *Tv. sulfidiphilus* ALJ17 and to *Tv. denitrificans* (Ahn et al., 2017; Sorokin et al., 2012). However, our cloning results of the biodesulfurization process sludge and finding of Sorokin et al. (2012) indicated that only *Tv. sulfidiphilus* is present in the lab- and full-scale installations (Kiragosyan et al., 2019b). We concluded that the designed primer set quantified well *Tv. sulfidiphilus* in the samples. In addition, we generated estimates of total bacterial 16S rRNA gene copy abundance by using the universal bacterial primer set 338f/518 r (Lane, 1991; Muyzer et al., 1993) to calculate relative target species abundances according to the quantification protocol described by Pallares-Vega et al. (2019).

2.5. Bacterial community analyses

Extracted DNA samples from each time point were amplified in triplicate by using barcoded forward primer 515f (5′-GTGYCAGCMG-CCGCGGTAA-3′) and reversed primer 926 r (5′−CCGYCAATTYMTTT-RAGTTT-3′). This primer set targets the V4-V5 variable region of the 16S rRNA gene (Parada et al., 2016). Amplification was done with the HotStarTaq Plus Master Mix Kit (Qiagen, USA) under the following

conditions: 94 °C for three minutes, followed by 30 cycles of 94 °C for 30 s, 53 °C for 40 s and 72 °C for one minute, with a final elongation step at 72 °C for five minutes. After amplification, the PCR products of the three separate reactions of each sample were pooled and checked on a 2% agarose gel to determine the success of the amplification process and the relative intensity of the bands. Next, multiple samples were pooled together (e.g., 100 samples) in equimolar amounts based on their molecular weight and DNA concentrations. Pooled samples were purified by using calibrated Ampure XP beads (Beckman Coulter, Indianapolis, IN, USA). MiSeq sequencing (2 × 300 bp) was performed at MR DNA (www.mrdnalab.com, Shallowater, TX, USA). Sequencing data were processed using the MR DNA analysis pipeline (MR DNA, Shallowater, TX, USA). In summary, barcodes were removed, and paired sequences were joined, after which sequences < 150bp and with ambiguous base calls were removed. Sequences were denoised, operational taxonomic units (OTUs) were generated and chimeras were removed. OTUs were defined by clustering at 3% divergence (97% similarity), and final OTUs were taxonomically classified using BLASTn against a curated database obtained from RDPII and NCBI (http://rdp.cme.msu.edu, www.ncbi.nlm.nih.gov). Demultiplexed sequences were submitted to the European Nucleotide Archive (ENA) EMBL-EBI under project number PRJEB32001.

2.6. Statistical analysis

16S rRNA sequencing data were analyzed in R studio (version 1.2.1335) using the Microbiome R package (Lahti et al., 2017). Only OTUs with a minimum of 100 reads in all samples were kept and total read abundance tables were used for statistical analysis. Ordination was done with multidimensional scaling (NMDS) and redundancy analyses (RDA) to find major trends in the microbial community.

To evaluate whether absolute qPCR-based bacterial count estimates were dependent on process conditions, we constructed a linear mixed-effects model to control for pseudo-replication of technical replicates. The linear mixed-effects model was constructed with 16S rRNA gene copies, process operation time, and their interaction as fixed effects and technical replicate as a random effect using the lme4 package (Bates et al., 2014) with R version 3.5.2. (R Core Team, 2018) in Rstudio software (version 1.1.456). Denominator degrees of freedom were approximated by using the Satterthwaite procedure in the lmer Test package (Kuznetsova et al., 2017) and species-specific temporal slope estimates were inferred using the *phia* package (de Rosario-Martinez, 2015). To assess the relationships between bacterial abundance and process performance parameters (sulfate, thiosulfate, and MT concentrations), we used linear regression analysis. For this analysis of variance, we used the average values of technical triplicates because we had only a single measurement of the process performance parameters for each sample.

2.7. Analytical techniques

A detailed description of the methods and techniques mentioned in Section 2.7 can be found in (Kiragosyan et al., 2020)

Biomass quantification was based on the amount of organically bound nitrogen oxidized to nitrate by digestion with peroxodisulfate (LCK238 and LCK338, Hach Lange, the Netherlands). Before analysis, the cell pellet was washed twice with nitrogen-free medium at 20,238 x g for 5 min to remove any residual urea and ammonia.

Sulfide was measured as total HS^- using a methylene-blue method in a cuvette test (LCK653, Hach Lange, USA). To assess whether the sulfur balance is closed, total S measurements were performed using inductively coupled plasma – optical emission spectrometry (ICP-OES, model, manufacturer location of manufacturer). The concentration of measured sulfur was compared with the sum of sulfate and thiosulfate (data and a full description can be found in Appendix A (in Supplementary material)).

Sulfate and thiosulfate were quantified by ion chromatography (Metrohm Compact IC 761, Switzerland) with an anion column (Metrohm Metrosep A Supp 5, 150/4.0 mm, Switzerland) equipped with a pre-column (Metrohm Metrosep A Supp 4/5 Guard, Switzerland). Before starting the analyses, most solids were removed by filtration over a 0.45-µm membrane syringe filter (HPF Millex, Merck, the Netherlands). To prevent chemical sulfide oxidation the filtered sample was subsequently mixed with 0.2 M zinc acetate in a 1:1 ratio to form ZnS. Afterward, the sample was centrifuged to separate ZnS and supernatant. In order to close the electron balance, cations Na^+, K^+ and total inorganic carbon were measured.

The biological sulfur concentration was calculated from the sulfur mass balance based on the supplied amount of sulfide and the actual sulfate and thiosulfate concentrations, according to:

$$[S^0]_t = (\Delta t(H_2S \text{ supplied})/ V_{liquid}) - [SO_4^{2-}]_t - 2*[S_2O_3^{2-}]_t - (S_x^{2-})_t, \quad (5)$$

in which the initial sulfur concentration is assumed to be zero. This is a general method to calculate the concentration of accumulated sulfur (De Rink et al., 2019; Klok et al., 2012; Roman et al., 2015; Van Den Bosch et al., 2009b). Concentrations of dissolved sulfide and possible volatile organosulfur compounds were not taken into account, as their combined concentrations relative to the total concentration of sulfur species is negligible (Van Den Bosch et al., 2009b). We also assume a pseudo steady-state condition of the system, which was confirmed by the consecutive liquid and gas samples (Kiragosyan et al., 2019a; Roman et al., 2016b; Van Den Bosch et al., 2008).

High-pressure liquid chromatography (HPLC) was used to determine dimethyl disulfide (DMDS), dimethyl trisulfide (DMTS), and organic polysulfides (dimethyl polysulfanes Me_2S_4 to Me_2S_8). For quantification of inorganic polysulfide anions (S_x^{2-}), they were derivatized to methyl polysulfanes with methyl trifluoromethanesulfonate (≥ 98% pure, Sigma-Aldrich, the Netherlands) as follows:

$$S_x^{2-} + 2CF_3SO_3Me \rightarrow Me_2S_x + 2CF_3SO_3\text{-} \quad (6)$$

The detailed sample preparation and derivatization procedures are described in Roman et al. (2014).

The gas phase (H_2S, N_2, CO_2, and O_2) was analyzed with a gas chromatograph (Varian CP4900 Micro GC, Agilent, the Netherlands) equipped with two separate column modules, namely a 10-m-long Mol Sieve 5A PLOT (MS5) and a 10-m-long PoraPlot U (PPU). The required sample volume was 3 mL.

Gaseous MT and DOPS concentrations were measured with a gas chromatograph (Thermo Scientific Trace GC Ultra with Trace GC Ultra valve oven, Interscience, Breda, the Netherlands) equipped with a Restek column (RT®-U-Bond, 30 m x0.53 mm di x20 µm df). Total sample volume was 3 mL to enable meticulous flushing. All tubing was of the type Sulfinert® to prevent absorption and reaction of the sulfur compounds.

The concentrations of MT and DOPS in the liquid phase were measured right after sample preparation with the same gas chromatograph that was used for the gaseous samples, but the injection was done to the liquid port. Sample preparation was followed by liquid-liquid extraction, for which we mixed each sample with n-hexane (Sigma-Aldrich, the Netherlands) and an internal standard from a stock solution in the ratio of 10:9:1 (sample:n-hexane:internal standard).

3. Results and discussion

3.1. Effect of methanethiol on process performance

During the first experimental run, the feed stream only consisted of H_2S to establish a stable baseline performance. After 15 days of stable process operation, we assessed the selectivity for sulfate, sulfur, and thiosulfate formation in the non-disturbed system. The selectivity for

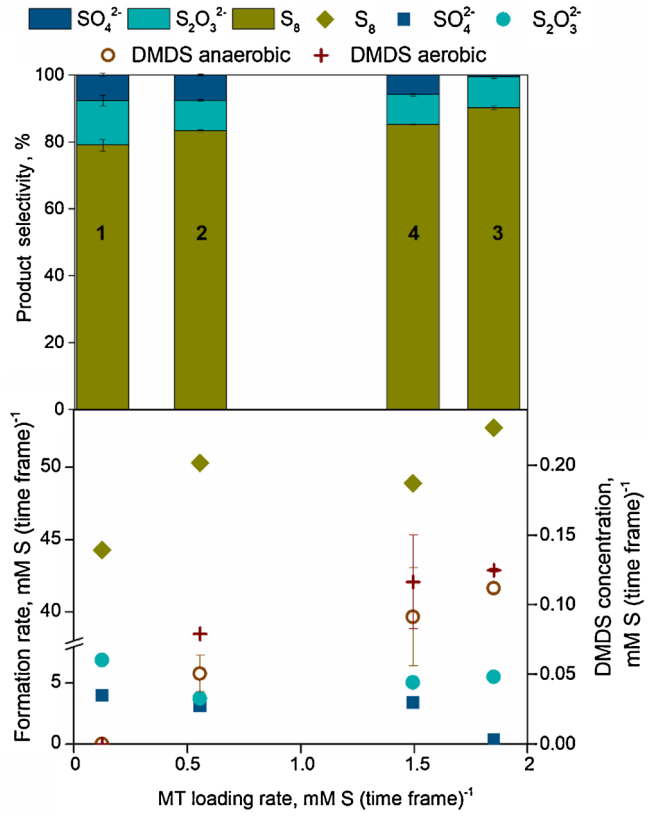

Fig. 2. Average product selectivity and formation rates of sulfate, thiosulfate, and dimethyl disulfide (DMDS) during lab-scale biodesulfurization process operation with addition of methanethiol (MT). MT loading rate is depicted in Fig. 3. The numbers in the green bars indicate the time frame: 1 = day 1–11, 2 = day 12–29, 3 = day 29–44, and 4 = day.44–47. (For interpretation of the references to colour in this figure legend, the reader is referred to the web version of this article.)

biologically produced sulfur and sulfate formation were 91.5 ± 1.2 mol % and 6.7 ± 1.1 mol%, respectively, and a relatively small amount of thiosulfate (1.8 ± 0.3 mol%) was formed. These selectivities are similar to the achieved sulfur selectivities in a traditional gas biodesulfurization setup consisting of a gas absorber and aerobic reactor (Kiragosyan et al., 2019a). During the second experiment, additional dosing of MT to the feed-gas was initiated over a 77-day period, during which the MT loading rate was gradually increased from 0 to 2 mM S day^{-1}.

In the experiment with MT addition, we calculated the average product selectivity for sulfate, thiosulfate, and sulfur per period, i.e. between every medium exchange (Fig. 2). At the start-up of the process (day 1–11), the sulfur selectivity was 79 mol%. This relatively low S production immediately after the process start-up resulted from increased levels of thiosulfate and sulfate selectivity (13 mol%, and 8 mol %, respectively), which indicates a limitation in the biological oxidation capacity (Kiragosyan et al., 2019a). After 12 days of operation, the sulfur selectivity slightly increased and reached the highest sulfur selectivity (90 mol%) during the highest MT loading (day 29 to 44). During days 45 to 77, the sulfur selectivity slightly dropped to 85 mol%, with 6 mol% of sulfate and 9 mol% of thiosulfate formation. Thiosulfate selectivity decreased and stabilized at 9 mol% for the rest of the experiment. The observed thiosulfate selectivity in the presence of MT is almost five times higher than in the experiment with H_2S only, i.e. 9 mol% vs. 1.8 mol%. One of the reasons is the decreased rate of biological (poly)sulfide oxidation by SOB in the presence of MT (Appendix B, Fig. B1 (in Supplementary material)). The biological sulfide oxidation rate decreased by a factor of three from 0.9 ± 0.04 to 0.3 ± 0.01 mM O_2 (mg N h)$^{-1}$ at 0.12 mM sulfide, after the SOB biomass had been exposed to MT for 77 days. The reduced biological oxidation capacity created more room for chemical sulfide oxidation, leading to the formation of thiosulfate, at elevated H_2S loading rates.

Conversely, more thiosulfate would form at constant H_2S loading upon increasing the MT dosing rates. Moreover, any biological thiosulfate oxidation will be suppressed in the presence of DODS (Kiragosyan et al., 2020; Roman et al., 2016c). To avoid thiosulfate formation in the presence of MT, it is recommended to start process operation with a higher SOB biomass concentration, i.e. ≥ 60 mg N L^{-1}.

In the biodesulfurization process, sulfate forms from sulfide and thiosulfate oxidation by SOB (Eqs. 2 and 6), although the specific oxidation rates for each substrate are different. In our previous studies, we found that the SOB oxidation rates of thiosulfate were three times lower than for sulfide oxidation, 0.09 ± 0.01 vs. 0.32 ± 0.02 mM O_2 (mg N h)$^{-1}$ (Kiragosyan et al., 2020). Hence, we assume that the primary source for sulfate formation was biological (poly)sulfide oxidation. The addition of MT has an inhibitory effect on sulfate formation. At MT loading rates below 1.4 mM S day^{-1}, the selectivity for sulfate formation was about 8 mol%, it started to decrease at higher MT loading rates (Fig. 2) and reached 0.6 mol% at the highest MT supply. Roman et al. (2016b) found that the sulfate selectivity was ~ 5 mol% with ~20 mol % of thiosulfate and 75 mol% of sulfur when MT was supplied to the system. Furthermore, we recently demonstrated that the product of MT oxidation – DMDS selectively inhibits sulfate formation (Kiragosyan et al., 2020). Formed sulfate can also affect the pH of the process medium and cause its acidification. Therefore, pH was monitored in both bioreactors and the difference between anaerobic and aerobic bioreactor was ~ 0.1. This small variation can be caused by the lower ORP of the process solution in the anaerobic bioreactor. But this 0.1 difference remained during the duration of the experiment.

In our latest experiments, the formed DMDS selectively inhibited sulfate formation as follows. There was a decrease in selectivity from 8 mol% to 0.6 mol% between 29 and 44 days and this triggered a slight increase in the thiosulfate formation rate (Fig. 2). This is in line with our previous findings (Kiragosyan et al., 2020). We also measured MT and other (diorgano)polysulfanes (tri- and tetrasulfides) in the bioreactor liquid, with GC-FPD. The second-most abundant DOPS was dimethyl trisulfide (DMTS). Dimethyl tetrasulfide was detected only in the last days of process operation, while no MT was detected (Appendix C, Fig. C1 (in Supplementary material)). In addition, the headspaces of both bioreactors and the gas outlet of the absorber were analyzed to detect any sulfur-containing gases. The concentration of DMDS in the headspace of the aerobic bioreactor and the gas outlet increased with increasing MT loading rate (Appendix C, Fig. C2 (in Supplementary material)). This dependency confirms that the liquid and gas phases were in pseudo-equilibrium. Roman et al. (2015) observed the same correlation in a traditional gas biodesulfurization system. In contrast to the DMDS concentration in the aerobic bioreactor, the anaerobic bioreactor headspace analysis showed a constant DMDS concentration independent of the MT loading rate (Appendix C, Fig. C2 (in Supplementary material)), indicating that the liquid and gaseous phases in the laboratory setup were in equilibrium. Furthermore, from our obtained results it follows that the anaerobic bioreactor dampens the supplied H_2S and also smoothens any ORP fluctuations resulting in a more stable O_2 supply rate. we hypothesize that reaction between sulfide and biosulfur occurs and polysulfides are formed.

In addition to DOPS, also inorganic polysulfides were detected in the bioreactor liquid (Eqs. 4 and 6). The average chain length of the polysulfides x_{av} was found to be 4.8 ± 0.2 S atoms (Fig. 3). This is in good agreement with the values reported by Roman et al. (2014). The sum of polysulfides was constant for about 25 days (0.6 ± 0.1 mM S) until the MT loading was increased to 2 mM S day^{-1}. The increase in the MT loading rate possibly triggered an increase in the sum of polysulfide species (Eq. 6) on days 29 to 44 and days 60 to 75; this was also observed by Roman et al. (2016a). As mentioned before, polysulfides

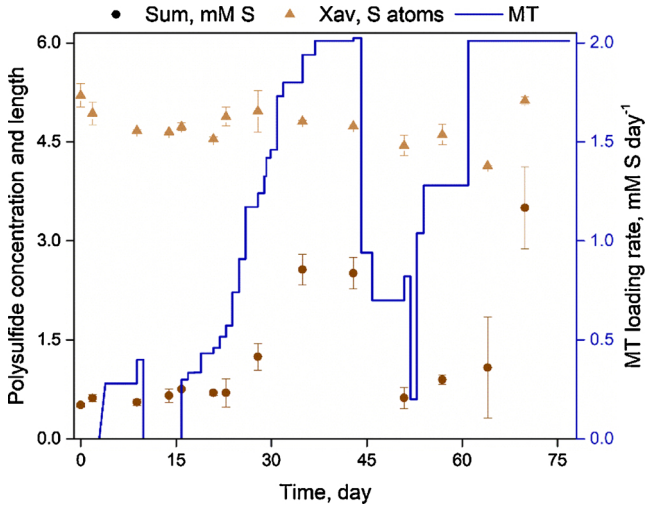

Fig. 3. Average sum of polysulfides and their length in the process liquid to supplied methanethiol (MT) loading rate to the lab-scale biodesulfurization setup. In correspondence to the time frames depicted in Fig. 2: 1 = day 1–11, 2 = day 12–29, 3 = day 29–44, and 4 = day.44–47.

are formed from the abiotic reaction between the produced bio-sulfur and sulfide (Eq. 4). Hence, the sulfide concentration in the liquid (at excess of elemental sulfur) was equivalent to the concentration of sulfane atoms of inorganic polysulfides (Appendix, A, Fig. A2 (in Supplementary material)). This indicates that all supplied sulfide immediately reacted with sulfur to form polysulfides. From this observation, we conclude that the actual electron donor in our lab-scale biodesulfurization setup was inorganic polysulfide, or, rather, its terminal sulfanes.

3.2. Effect of methanethiol on sulfur-oxidizing bacterial community dynamics

The biomass grown in the experiment fed with sulfide alone was subsequently used as inoculum for the experiment with H_2S and MT as feed gases. The relative abundance and absolute 16S rRNA copy number (qPCR) of the dominant SOB species (*Alkalilimnicola ehrlichii*, *Thioalkalivibrio sulfidiphilus,* and *Thioalkalibacter halophilus*) were similar at the end of the experiment with sulfide and at the beginning of the experiment with sulfide + MT (Fig. 4). From the results of 16S amplicon sequencing and qPCR, it appears that the presence of MT provided a competitive advantage to a SOB population closely related to the extremely salt-tolerant and facultatively alkaliphilic *Thioalkalibacter halophilus* (Banciu et al., 2008), with a significant increase in its 16S rRNA log copies number ($p = 3.814*10^{-16}$). Interestingly, the same SOB species was also reported as dominant in a previous study on thiols (Roman et al., 2016b). The presence of DMDS (as a product of chemical MT oxidation, Eq. 4) but not the MT itself proved to be a direct factor for the proliferation of *Thb. halophilus*, as has been shown before (Kiragosyan et al., 2020). The second in abundance was a SOB population closely related to haloalkaliphilic *Alkalilimnicola ehrlichii*, which became dominant in the MT-free experiment and was still dominant at a moderate MT supply. However, on day 44, when the highest MT loading rate was reached (2 mM S day^{-1}), the relative abundance of *Alkalilimnicola* dropped drastically (Fig. 4B). Intoxication of the SOB with MT/DMDS and competition with a more thiol-adapted and DMDS-resistant (IC_{50} = 2.37 ± 0.1 mM) *Thioalkalibacter* could be the cause of this (Kiragosyan et al., 2020).

Moreover, MT also influenced less dominant members of the initial bacterial community at the highest loading of 2 mM S day^{-1} at day 29 (Appendix D, Fig. D1 (in Supplementary material)). These included the gammaproteobacterial genera *Thioalkalimicrobium*, *Halomonas* and *Thioalkalivibrio. Halomonas* species are aerobic or facultative anaerobic chemoorganotrophic halo(alkali)philes utilizing a wide range of organic substrates (such as fatty acids and sugars, but also hydrocarbons) that can oxidize inorganic sulfur compounds incompletely to tetrathionate (García et al., 2005; Sorokin, 2003). From the start of the first experiment, the relative abundance of *Halomonas* declined and continued to decrease with the introduction of MT. A possible explanation is the low concentration of available organics in the feed gas and the inability of *Halomonas* to withstand methanethiol toxicity (Van Den Bosch et al., 2009a). The genera *Thioalkalivibrio* and *Thioalkalimicrobium* are obligate chemolithoautotrophic haloalkaliphilic SOB that dominate in natural soda lakes (Sorokin et al., 2013; Vavourakis et al., 2018). The relative abundance of *Thioalkalimicrobium* and *Thioalkalivibrio* was constant when only sulfide was supplied, whereas in the experiment with additional MT supply, the relative abundance of *Thioalkalimicrobium* decreased drastically within the first ten days of process operation with MT supply. In addition, the relative abundance of *Thioalkalivibrio* decreased from 14 to 1.8% during the first 29 days of process operation and reached a minimum on day 44, at the highest MT supply. The most probable explanation for the apparent low tolerance of *Tv. sulfidiphilus* to thiols is the fact that its only cytochrome oxidase is of the cbb_3 type, which is highly sensitive to inhibition by organic sulfur compounds (Kiragosyan et al., 2020; Roman et al., 2016a, 2016c, 2015; Van Den Bosch et al., 2009a). The drop in the abundance of *Tv. sulfidiphilus* provided an advantage for the growth of *Thb. halophilus* and *Alk. ehrlichii*. As the results from the 16S amplicon sequencing cannot answer questions on species interaction and dynamics, we performed qPCR analyses to monitor growth dynamics and establish absolute 16S rRNA counts of the three SOB key players: *Thb. halophilus*, *Tv. sulfidiphilus* and *Alk. ehrlichii*.

The qPCR results showed that throughout process operation, the absolute abundance of *Thb. halophilus* rRNA increased by 2 log copies $(ng\ DNA)^{-1}$, whereas *Thioalkalivibrio sulfidiphilus* had decreased by 2.3 log copies $(ng\ DNA)^{-1}$ by the end of the process operation with MT (Fig. 3B). These estimates of absolute abundance confirm the observed pattern of relative abundances of the genera *Thioalkalibacter* and *Thioalkalivibrio* obtained from the 16S rRNA gene amplicon sequencing. However, while the absolute abundance of *Alk. ehrlichii* only decreased by about 0.6 log copies $(ng\ DNA)^{-1}$, its relative abundance decreased by 46% when the highest concentration of MT was reached (2 mM S day^{-1}) (Fig. 4B). The absolute quantity of total bacterial 16S rRNA log copies $(ng\ DNA)^{-1}$ remained almost constant over the first 29 days of process operation, with only a slight decline at a high MT concentration. These seemingly discrepant estimates of *Alk. ehrlichii* between qPCR and amplicon sequencing might have originated from the difference in *Alk. ehrlichii*-specific amplification efficiencies of the universal 335 F/518R primer set (amplicon sequencing) and the highly species-specific primer set (qPCR) (Leray et al., 2013). Moreover, this discrepancy may further be enhanced by primer binding competition and PCR bias as 16S rRNA amplicon sequence counts depend on the presence in the sample of other species, especially those closely related to the target (Snyder et al., 2009). This problem is thus particularly pertinent for relatively less abundant species. In contrast to 16S amplicon sequencing, the qPCR outcome does not depend on the abundance of other detected species and is conventionally used as a proxy for the absolute bacterial count (Bonk et al., 2018).

We further analyzed a possible correlation between the SOB key species and process performance parameters, including sulfate and thiosulfate concentrations, as well as MT loading rate, to evaluate whether these SOBs were responsible for sulfate and thiosulfate formation. After we corrected for pseudo-replication and the accumulation of thiosulfate and sulfate, the methanethiol loading rate was the main contributing factor to the species' absolute counts (Appendix E, Figs. E1 and E2 (in Supplementary material)). MT concentration predicted species growth and lapse: MT positively affected *Thb. halophilus* growth (lmer Bonferroni adjustment, $p = 2 \times 10^{-16}$), whereas MT negatively affected the growth of *Tv. sulfidiphilus* (lmer Bonferroni adjustment, p =

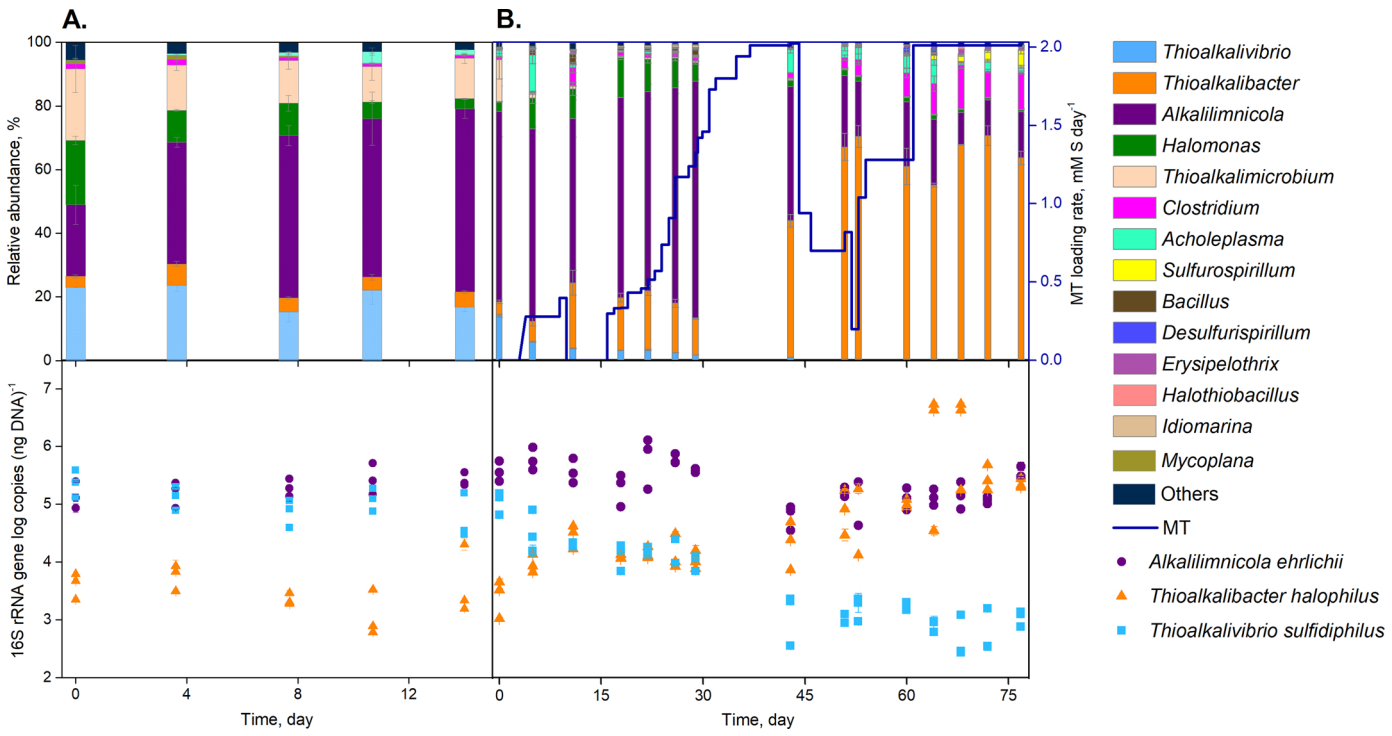

Fig. 4. The relative abundance of the microbial composition (top) and quantified 16S rRNA gene copies (bottom) of *Thioalkalivibrio sulfidiphilus*, *Thioalkalibacter halophilus,* and *Alkalilimnicola ehrlichii* during (A) H_2S and (B) H_2S + stepwise increased supply of methanethiol (MT). Only bacteria with a relative abundance higher than 0.5% are listed; remaining species are clustered into "Others". Relative abundance results represent the average value, and the error bars represent the standard deviation of the three biological replicates. 16S rRNA gene log copies are an average value of the measured technical duplicates, whereas each data point is a biological replicate at each time point. The error bars indicate the standard deviation between the technical duplicates. The lab-scale gas biodesulfurization bioreactor system was operated at a low oxidation-reduction potential of −390 mV, pH 8.5, and the H_2S loading rate was 58.12 mM S day^{-1}. In correspondence to the time frames depicted in Fig. 2: 1 = day 1–11, 2 = day 12–29, 3 = day 29–44, and 4 = day 44.

2×10^{-16}) and *Alk. ehrlichii* (lmer Bonferroni adjustment, p = 0.04) (Fig. E1). These results are in concordance with our previous study, in which *Thb. halophilus* abundance rapidly increased within five days of DMDS addition, while the growth dynamics of *Tv. sulfidiphilus* and *Alk. ehrlichii* did not change from the inoculum stage (Kiragosyan et al., 2020). The difference in growth dynamics of the SOB key species between the MT- and DMDS-supplied experiments likely depends on the differential toxicity of these compounds and their effects on bacterial activity. MT is known as a competitive inhibitor for the bacterial sulfide oxidation, while DMDS is non-competitive (Appendix C, Fig.C1 (in Supplementary material)) (Roman et al., 2016c). Furthermore, With the addition of anaerobic bioreactor, it was postulated that selective pressure for SOB is created to stimulate the growth of SOB that oxidizes sulfide to sulfur mainly or only from sulfur. To support this hypothesis, we monitored SOB community change and the growth of three key-species. However, gene expression and involved enzymes in the sulfide oxidation process need to be studied in a follow-up study.

In both the present study and the previous study, *Thb. halophilus* proliferation was enhanced in the presence of thiols. We believe this is because of the presence of the quinol oxidase *bd* in addition to cytochrome c oxidase cbb_3 (according to the genomic data) in this SOB species (Sorokin et al., 2020). The former is known to be much more resistant to various inhibitors binding to the heme-Cu family cytochrome oxidases (Quesada et al., 2007). As a comparison, inhibitor-sensitive cytochrome oxidase cbb_3 (heme-Cu family) is the only oxidase present in the genome of *Tv. sulfidiphilus* and other dominant SOB species in gas biodesulfurization systems (Muyzer et al., 2011; Roman et al., 2015). These results provide valuable information on the application and use of *Thioalkalibacter halophilus* species in gas biodesulfurization systems for achieving high sulfur selectivity and stable process operation in the presence of thiols. More research is needed to understand the effect of thiols on the overall pathways of sulfide oxidation in these bacteria.

4. Conclusions

Addition of an anaerobic bioreactor to a traditional gas biodesulfurization lineup resulted in increased sulfur formation during addition of MT. Sulfur selectivity increased up to 90 mol% in comparison to 75 mol% in the traditional lineup. During process operation with MT addition, the lowest observed sulfate selectivity was 0.6 mol%, resulting from selective inhibition of sulfate formation by chemically formed DMDS from MT oxidation. We also found that all supplied sulfide was converted into polysulfides, which served as the actual electron donor for biological (poly)sulfide oxidation.

The changes in process performance were accompanied by changes in the SOB community composition. In a traditional biodesulfurization systems with only H_2S present in the feed gas, *Thioalkalivibrio sulfidiphilus* is the dominant SOB in most of the cases (Kiragosyan et al., 2019a; Sorokin et al., 2012, 2008). In the dual bioreactor lineup, however, we found that *Alkalilimnicola ehrlichii* became the dominant organism when H_2S was the only feed gas. In the presence of MT, *Thioalkalibacter halophilus* became the most abundant haloalkaliphilic SOB species. These shifts in SOB community composition and changes in the dynamics of SOB key species likely depend on the increasingly low redox potential in the presence of the anaerobic reactor (selective for *Alkalilimnicola*) and differential toxicity of organic sulfur compounds, i.e MT and DMDS, and their effects on the SOB activity (selective for *Thioalkalibacter*). The overall outcome of this work is a deeper understanding of microbial sulfide oxidation and community composition dynamics in a gas biodesulfurization process for H_2S and methanethiol. Furthermore, we have identified the MT-resistant SOB

population, which ensures stable sulfide removal in the presence of high MT concentrations with 90 mol% of sulfur formation.

Author statement

Karine Kiragosyan conceived and designed the analyzes, performed the analysis, collected the data, and wrote the publication. Magali Picard assisted with bioreactor operation and sample analysis. Peer H.A Timmers facilitated microbial community data analysis. Dimitry Y. Sorokin and Johannes B.M. Klok contributed with fruitful discussions and writing. Pawel Roman participated in the design of the experimental work, guided through sample analysis, and contributed with writing. Albert J.H. Janssen contributed with guidance and contributed to writing.

Declaration of Competing Interest

The authors declare that they have no known competing financial interests or personal relationships that could have appeared to influence the work reported in this paper.

Acknowledgments

This work has been performed within the cooperation framework of Wetsus, European Centre of Excellence for Sustainable Water Technology (wetsus.nl), Wageningen University and Research (wur.nl) and Paqell B.V. (paqell.com). Wetsus is co-funded by the Netherlands' Ministry of Economic Affairs and Ministry of Infrastructure and Environment, the European Union's Regional Development Fund, the Province of Fryslân and the Northern Netherlands Provinces. Wetsus is also a coordinator of the WaterSEED project, which received funding from European Union's Horizon 2020 research and innovation program under Marie Skłodowska-Curie grant agreement No. 665874. The research of Peer H.A. Timmers and Dimitry Sorokin was supported by the Soehngen Institute of Anaerobic Microbiology (SIAM) Gravitation grant (024.002.002) of the Netherlands Ministry of Education, Culture, and Science and the Netherlands Organisation for Scientific Research (NWO). Dimitry Sorokin was also supported by the Wetsus consultancy project. We thank Pieter van Veelen for his guidance and help with the statistical analyses.

Appendix A. Supplementary data

Supplementary material related to this article can be found, in the online version, at doi:https://doi.org/10.1016/j.jhazmat.2020.123002.

References

Ahn, A.-C., Overmars, L., Sorokin, D.Y., Meier-Kolthoff, J.P., Muyzer, G., Richter, M., Woyke, T., 2017. Genomic diversity within the haloalkaliphilic genus *Thioalkalivibrio*. PLoS One 12, e0173517. https://doi.org/10.1371/journal.pone.0173517.

Banciu, H.L., Sorokin, D.Y.Y., Tourova, T.P., Galinski, E.A., Muntyan, M.S., Kuenen, J.G., Muyzer, G., 2008. Influence of salts and pH on growth and activity of a novel facultatively alkaliphilic, extremely salt-tolerant, obligately chemolithoautotrophic sufur-oxidizing Gammaproteobacterium*Thioalkalibacter halophilus* gen. nov., sp. nov. from South-Western Siber. Extremophiles 12, 391–404. https://doi.org/10.1007/s00792-008-0142-1.

Bates, D., Mächler, M., Bolker, B., Walker, S., 2014. Fitting Linear Mixed-effects Models Using lme4. https://doi.org/10.18637/jss.v067.i01.

Bonk, F., Popp, D., Harms, H., Centler, F., 2018. PCR-based quantification of taxa-specific abundances in microbial communities: quantifying and avoiding common pitfalls. J. Microbiol. Methods 153, 139–147. https://doi.org/10.1016/j.mimet.2018.09.015.

Chen, M., Yao, X.Z., Ma, R.C., Song, Q.C., Long, Y., He, R., 2017. Methanethiol generation potential from anaerobic degradation of municipal solid waste in landfills. Environ. Sci. Pollut. Res. 24, 23992–24001. https://doi.org/10.1007/s11356-017-0035-x.

Cline, C., Hoksberg, A., Abry, R., Janssen, A., 2003. Biological process for H2S removal from gas streams: the Shell-paques / thiopaq ™ gas desulfurization process. Proc. Laurance Reid Gas Cond. Conf. 1–18.

De Rink, R., Klok, J.B.M., Sorokin, D.Y., Van Heeringen, G.J., Ter Heijne, A., Zeijlmaker, R., Mos, Y.M., De Wilde, V., Keesman, K.J., Buisman, C.J.N., 2019. Increasing the selectivity for sulfur formation in biological gas desulfurization. Environ. Sci. Technol. 53, 4519–4527. https://doi.org/10.1021/acs.est.8b06749.

de Rosario-Martinez, H., 2015. Phia: Post-hoc Interaction Analysis. R Package Version 0.2-1. [WWW Document]. URL. https://cran.r-project.org/package=phia.

García, M.T., Ventosa, A., Mellado, E., 2005. Catabolic versatility of aromatic compound-degrading halophilic bacteria. FEMS Microbiol. Ecol. 54, 97–109. https://doi.org/10.1016/j.femsec.2005.03.009.

Kiragosyan, K., Klok, J.B.M., Keesman, K.J., Roman, P., Janssen, A.J.H., 2019a. Development and validation of a physiologically based kinetic model for starting up and operation of the biological gas desulfurization process under haloalkaline conditions. Water Res. X 4, 100035. https://doi.org/10.1016/j.wroa.2019.100035.

Kiragosyan, K., Picard, M., Sorokin, D.Y., Dijkstra, J., Klok, J.B.M., Roman, P., Janssen, A.J.H., 2020. Effect of dimethyl disulfide on the sulfur formation and microbial community composition during the biological H2S removal from sour gas streams. J. Hazard. Mater. 386. https://doi.org/10.1016/j.jhazmat.2019.121916.

Kiragosyan, K., van Veelen, P., Gupta, S., Tomaszewska-Porada, A., Roman, P., Timmers, P.H.A., 2019b. Development of quantitative PCR for the detection of *Alkalilimnicola ehrlichii*, *Thioalkalivibrio sulfidiphilus* and *Thioalkalibacter halophilus* in gas biodesulfurization processes. AMB Express 9, 99. https://doi.org/10.1186/s13568-019-0826-1.

Klok, J.B.M., de Graaff, M., van den Bosch, P.L.F., Boelee, N.C., Keesman, K.J., Janssen, A.J.H., 2013. A physiologically based kinetic model for bacterial sulfide oxidation. Water Res. 47, 483–492. https://doi.org/10.1016/j.watres.2012.09.021.

Klok, J.B.M., Van Den Bosch, P.L.F., Buisman, C.J.N., Stams, A.J.M., Keesman, K.J., Janssen, A.J.H., 2012. Pathways of sulfide oxidation by haloalkaliphilic bacteria in limited-oxygen gas lift bioreactors. Environ. Sci. Technol. 46, 7581–7586. https://doi.org/10.1021/es301480z.

Kuznetsova, A., Brockhoff, P.B., Christensen, R.H.B., 2017. lmerTest Package: Tests in Linear Mixed Effects Models. J. Stat. Softw. 82. https://doi.org/10.18637/jss.v082.i13.

Lahti, L., Shetty, S., Obenchain, V., Salojärvi, J., Gilmore, R., Blake, T., Turaga, N., Pagès, H., Ramos, M., Salosensaari, A., 2017. Tools for Microbiome Analysis in R.

Lane, D.J., 1991. 16S/23S rRNA sequencing. In: Stackebrandt, E., Goodfellow, M. (Eds.), Nucleic Acid Techniques in Bacterial Systematic. John Wiley & Sons, Inc., New York, pp. 115–175.

Leray, M., Yang, J.Y., Meyer, C.P., Mills, S.C., Agudelo, N., Ranwez, V., Boehm, J.T., Machida, R.J., 2013. A new versatile primer set targeting a short fragment of the mitochondrial COI region for metabarcoding metazoan diversity: Application for characterizing coral reef fish gut contents. Front. Zool. 10, 1–14. https://doi.org/10.1186/1742-9994-10-34.

Muyzer, G., Sorokin, D.Y., Mavromatis, K., Lapidus, A., Clum, A., Ivanova, N., Pati, A., D'Haeseleer, P., Woyke, T., Kyrpides, N.C., 2011. Complete genome sequence of "*Thioalkalivibrio sulfidophilus*" HL-EbGr7. Stand. Genomic Sci. 4, 23–35. https://doi.org/10.4056/sigs.1483693.

Muyzer, G., Waal, E.C.D.E., Uitierlinden, A.G., 1993. Profiling of Complex Microbial Populations by Denaturing Gradient Gel Electrophoresis Analysis of Polymerase Chain Reaction-Amplified Genes Coding for 16S rRNA. Appl. Environ. Microbiol. 59, 695–700.

Pallares-Vega, R., Blaak, H., van der Plaats, R., de Roda Husman, A.M., Leal, L.H., van Loosdrecht, M.C.M., Weissbrodt, D.G., Schmitt, H., 2019. Determinants of presence and removal of antibiotic resistance genes during WWTP treatment: a cross-sectional study. Water Res. https://doi.org/10.1016/j.watres.2019.05.100.

Parada, A.E., Needham, D.M., Fuhrman, J.A., 2016. Every base matters: Assessing small subunit rRNA primers for marine microbiomes with mock communities, time series and global field samples. Environ. Microbiol. 18, 1403–1414. https://doi.org/10.1111/1462-2920.13023.

Quesada, A., Guijo, M.I., Merchan, F., Blazquez, B., Igeno, M.I., Blasco, R., 2007. Essential Role of Cytochrome bd-Related Oxidase in Cyanide Resistance of*Pseudomonas pseudoalcaligenes* CECT5344. Appl. Environ. Microbiol. 73, 5118–5124. https://doi.org/10.1128/aem.00503-07.

R Core Team, 2018. R: a Language and Environment for Statistical Computing. [WWW Document]. R Found. Stat. Comput., Vienna, Austria.

Roman, P., Bijmans, M.F.M., Janssen, A.J.H., 2016a. Influence of methanethiol on biological sulphide oxidation in gas treatment system. Environ. Technol. 3330, 1–11. https://doi.org/10.1080/09593330.2015.1128001.

Roman, P., Bijmans, M.F.M., Janssen, A.J.H., 2014. Quantification of individual polysulfides in lab-scale and full-scale desulfurisation bioreactors. Environ. Chem. 11, 702–708. https://doi.org/10.1071/EN14128.

Roman, P., Klok, J.B.M., Sousa, J.A.B., Broman, E., Dopson, M., Van Zessen, E., Bijmans, M.F.M., Sorokin, D.Y., Janssen, A.J.H., 2016b. Selection and Application of Sulfide Oxidizing Microorganisms Able to Withstand Thiols in Gas Biodesulfurization Systems. Environ. Sci. Technol. https://doi.org/10.1021/acs.est.6b04222. acs.est.6b04222.

Roman, P., Lipińska, J., Bijmans, M.F.M., Sorokin, D.Y., Keesman, K.J., Janssen, A.J.H., 2016c. Inhibition of a biological sulfide oxidation under haloalkaline conditions by thiols and diorgano polysulfanes. Water Res. 101, 448–456. https://doi.org/10.1016/j.watres.2016.06.003.

Roman, P., Veltman, R., Bijmans, M.F.M., Keesman, K.J., Janssen, A.J.H., 2015. Effect of Methanethiol Concentration on Sulfur Production in Biological Desulfurization Systems under Haloalkaline Conditions. Environ. Sci. Technol. 49, 9212–9221. https://doi.org/10.1021/acs.est.5b01758.

Smet, E., Lens, P., Van Langenhove, H., 1998. Treatment of waste gases contaminated with odorous sulfur compounds. Crit. Rev. Environ. Sci. Technol. 28, 89–117. https://doi.org/10.1080/10643389891254179.

Snyder, L.A.S., Loman, N., Pallen, M.J., Penn, C.W., 2009. Next-generation sequencing - the promise and perils of charting the great microbial unknown. Microb. Ecol. 57, 1–3. https://doi.org/10.1007/s00248-008-9465-9.

Sorokin, D.Y., 2003. Oxidation of inorganic sulfur compounds by obligately organotrophic bacteria. Microbiology 72, 641–653. https://doi.org/10.1023/B:MICI.0000008363.24128.e5.

Sorokin, D.Y., Merkel, A.Y., Muyzer, G., 2020. Genus *thioalkalibacter*. Bergey's Manual of Systematics of Archaea and Bacteria. John Wiley & Sons, Inc.https://doi.org/10.1002/9781118960608.gbm01692.

Sorokin, D.Y., Muntyan, M.S., Panteleeva, A.N., Muyzer, G., 2012. *Thioalkalivibrio sulfidiphilus* sp. nov., a haloalkaliphilic, sulfur-oxidizing gammaproteobacterium from alkaline habitats. Int. J. Syst. Evol. Microbiol. 62, 1884–1889. https://doi.org/10.1099/ijs.0.034504-0.

Sorokin, D.Y., Van Den Bosch, P.L.F., Abbas, B., Janssen, A.J.H., Muyzer, G., 2008. Microbiological analysis of the population of extremely haloalkaliphilic sulfur-oxidizing bacteria dominating in lab-scale sulfide-removing bioreactors. Appl. Microbiol. Biotechnol. 80, 965–975. https://doi.org/10.1007/s00253-008-1598-8.

Syed, M., Soreanu, G., Falletta, P., Béland, M., 2006. Removal of hydrogen sulfide from gas streams using biological processes - A review. Can. Biosyst. Eng. 48, 1–14.

Ter Heijne, A., De Rink, R., Liu, D., Klok, J.B.M., Buisman, C.J.N., 2018. Bacteria as an Electron shuttle for sulfide oxidation. Environ. Sci. Technol. Lett. 5, 495–499. https://doi.org/10.1021/acs.estlett.8b00319.

Van Den Bosch, P.L.F., De Graaff, M., Fortuny-Picornell, M., Van Leerdam, R.C., Janssen, A.J.H., 2009a. Inhibition of microbiological sulfide oxidation by methanethiol and dimethyl polysulfides at natron-alkaline conditions. Appl. Microbiol. Biotech. 83, 579–587. https://doi.org/10.1007/s00253-009-1951-6.

Van Den Bosch, P.L.F., Fortuny-Picornell, M., Janssen, A.J.H., 2009b. Effects of Methanethiol on the Biological Oxidation of Sulfide at Natron-Alkaline Conditions. Environ. Sci. Technol. 43, 453–459. https://doi.org/10.1021/es801894p.

Van Den Bosch, P.L.F., Sorokin, D.Y., Buisman, C.J.N., Janssen, A.J.H., 2008. The effect of pH on thiosulfate formation in a biotechnological process for the removal of hydrogen sulfide from gas streams. Environ. Sci. Technol. 42, 2637–2642. https://doi.org/10.1021/es7024438.

Van Den Bosch, P.L.F., Van Beusekom, O.C.C., Buisman, C.J.N., Janssen, A.J.H., 2007. Sulfide Oxidation at Halo-Alkaline Conditionsin a Fed-Batch Bioreactor. Biotechnol. Bioeng. 97, 1053–1063. https://doi.org/10.1002/bit.

Vavourakis, C.D., Andrei, A.-S., Mehrshad, M., Ghai, R., Sorokin, D.Y., Muyzer, G., 2018. A metagenomics roadmap to the uncultured genome diversity in hypersaline soda lake sediments. Microbiome 6, 168. https://doi.org/10.1186/s40168-018-0548-7.